Quantum Electronics **39** (12) 1165 – 1168 (2009)

PHOTODETECTORS

PACS numbers: 42.60.Da; 42.82.Et; 85.60.Gz
DOI: 10.1070/QE2009v039n12ABEH014148

Microcavity array IR photodetector

A.K. Esman, V.K. Kuleshov, G.L. Zykov

***Abstract*. An original microcavity array IR photodetector is proposed and the sensitivity and response time of its pixels are calculated. A photosensitive element represents a composite silicon microcavity made of two optically coupled closed waveguides on a dielectric substrate whose resonance wave depends on its temperature. This dependence is used to detect IR radiation which heats an absorbing element and the composite microcavity thermally coupled with this element. It is shown that for a spatial resolution of 45 μm, the time response is 30 ms and the sensitivity is 10^{-3} K at the IR radiation power of $\sim 4.7 \times 10^{-8}$ W element^{-1}.**

Keywords: *array IR image converter, composite microcavity, laser, photodetector.*

1. Introduction

Increasing interest in using infrared imaging for solving a variety of scientific and applied problems stimulates the search for new methods of converting IR images to the visible region and the investigation of array IR photodetectors featuring better operating parameters at a lower cost [1, 2].

At present intensive research works are under way toward the development of IR radiation converters for various applications. First of all, this is explained by the fact that the field of practical applications of infrared imaging devices and systems steadily expands due to the use of new and improvement of known array IR image converters.

The main parameters of array IR devices are the sensitivity of the array converter element, which determines the minimal temperature drop that can be detected, and the time constant determining the response time of the IR detector.

In this paper, we consider an original microcavity array IR photodetector, which can be used for the development of IR converters of a new type [3]. As a photosensitive element, we propose to use a composite microcavity consisting of two optically coupled closed waveguides on a dielectric substrate whose resonance wavelength depends on its temperature. This dependence, as will be shown below, is used to detect IR radiation that heats the absorbing element and the composite microcavity thermally coupled with it.

A.K. Esman, V.K. Kuleshov, G.L. Zykov B.I. Stepanov Institute of Physics, National Academy of Sciences of Belarus, prosp. Nezavisimosti 68, 220072 Minsk, Belarus; e-mail: lomoi@inel.bas-net.by

Received 5 May 2009; revision received 3 August 2009
Kvantovaya Elektronika **39** (12) 1165 – 1168 (2009)
Translated by M.N. Sapozhnikov

2. Operation principle of a microcavity array IR photodetector

We consider the operation of the IR photodetector by the example of functioning of one of its pixels (Fig. 1). In the initial state, when IR radiation does not fall on the photodetector, substrate (*1*) and all the elements located on it have temperature T_0 of the environment. The radiation frequency of tunable waveguide laser (*7*) is set equal to the resonance frequency of composite microcavity (*14*) made of optically coupled closed waveguides (*9*) and (*10*) [4]. For this purpose, besides the injection current flowing through active medium (*3*) of laser (*7*), the electric bias voltage is fed to its output Bragg reflector (*4*) via electrodes (*6*), at which radiation of this laser from input waveguide (*8*), according to the optical coupling coefficient, is coupled successively to closed waveguides (*9*) and (*10*). The optical coupling coefficient k_1 of waveguides (*8*) and (*9*) is specified by the width of the gap between them and the length of the interaction region of these elements and can be chosen considerably smaller than unity. Because of this, only a small part of the output optical power of laser (*7*) is used for the operation of one pixel of the IR array, while the rest of the output radiation power can be directed on the inputs of other pixels. In output waveguide (*12*) an optical signal appears at the laser frequency with the amplitude determined by the value of the resonance characteristic of composite microcavity (*14*) at this frequency. Infrared radiation of power P is focused by optical system (*15*) on absorbing element (*11*). As a result, the temperature and linear size of absorbing element (*11*) and both closed waveguides (*9*) and (*10*) of composite microcavity (*14*) begin to change because all these elements are in a thermal contact. This leads to the frequency shift of the resonance absorption band of microcavity (*14*) with respect to its initial position. The part of the output power of laser (*7*) entering to output waveguide (*12*) from closed waveguide (*10*) depends on the value of this shift. Therefore, the amplitudes of the optical signal in waveguide (*12*) and of the corresponding output electric signal of photodetector (*13*) change.

The dependences of the change in the part of the output power of laser (*7*) entering to microcavity (*14*) from input waveguide (*8*) and transmitted then to output waveguide

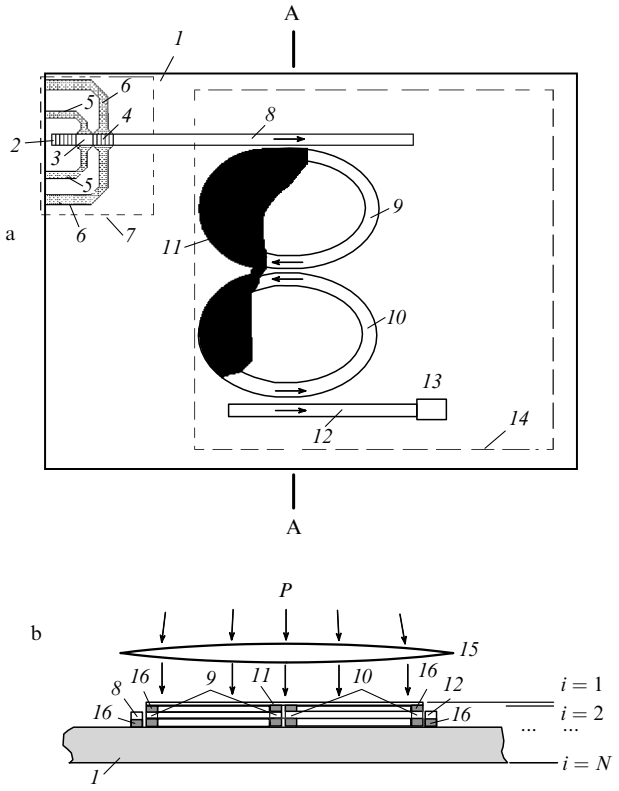

Figure 1. Schematic view of pixel elements (a) and the cross section of composite microcavity (*14*) along the AA line in Fig. 1a (b): (*1*) substrate; (*2, 4*) Brag reflectors; (*3*) active laser medium; (*5, 6*) electrodes for delivering the injection current and applying the bias voltage; (*7*) waveguide laser; (*8, 12*) input and output waveguides; (*9, 10*) closed waveguides; (*11*) absorbing element; (*13*) photodetector; (*14*) composite microcavity; (*15*) optical system (for example, objective); (*16*) buffer layers; *i* is a layer number.

(*12*) on the shift of the resonance wavelength of the microcavity and optical coupling coefficients were determined by mathematical simulations.

3. Analysis of the main parameters of a photosensitive element

We will estimate the main parameters of one pixel of the IR photodetector formed by successively coupled linear (*8*, *12*) and closed (*9*, *10*) waveguides by considering only one TM component E_z of the wave, for which the D'Alembert equation is valid [5]. The transient characteristics of the photosensitive element were numerically simulated based on two-dimensional D'Alembert equations in Cartesian coordinates x, y for straight waveguides (*8*) and (*12*) and in cylindrical coordinates ρ, φ for closed waveguides (*9*) and (*10*):

$$\frac{\partial^2 E_z}{\partial x^2} + \frac{\partial^2 E_z}{\partial y^2} - \frac{n_w^2}{c^2}\frac{\partial^2 E_z}{\partial t^2} = 0, \tag{1}$$

$$\frac{1}{\rho}\frac{\partial}{\partial \rho}\left(\rho \frac{\partial E_z}{\partial \rho}\right) + \frac{1}{\rho^2}\frac{\partial^2 E_z}{\partial \varphi^2} - \frac{n_r^2}{c^2}\frac{\partial^2 E_z}{\partial t^2} = 0, \tag{2}$$

where n_w and n_r are the effective refractive indices of materials of input (*8*) and output (*12*) waveguides and closed waveguides (*9*) and (*10*), respectively; c is the speed of light in vacuum; and t is time.

Equations (1) and (2) were supplemented with initial and boundary conditions. Calculations by these equations were performed by using the explicit numerical 'cross' scheme [6]. The spatial and time derivatives in wave equations (1) and (2) had the form

$$\frac{\partial^2 E_z}{\partial x^2} \approx \frac{E_z(x_{l+1}, y_m, t_n) - 2E_z(x_l, y_m, t_n) + E_z(x_{l-1}, y_m, t_n)}{(\Delta x)^2},$$

$$\frac{\partial^2 E_z}{\partial y^2} \approx \frac{E_z(x_l, y_{m+1}, t_n) - 2E_z(x_l, y_m, t_n) + E_z(x_l, y_{m-1}, t_n)}{(\Delta y)^2}, \tag{3}$$

$$\frac{\partial^2 E_z}{\partial t^2} \approx \frac{E_z(x_l, y_m, t_{n+1}) - 2E_z(x_l, y_m, t_n) + E_z(x_l, y_m, t_{n-1})}{(\Delta t)^2},$$

$$\frac{\partial E_z}{\partial \rho} \approx \frac{E_z(\rho_{l+1}, \varphi_m, t_n) - E_z(\rho_l, \varphi_m, t_n)}{\Delta \rho},$$

$$\frac{\partial^2 E_z}{\partial \rho^2} \approx \frac{E_z(\rho_{l+1}, \varphi_m, t_n) - 2E_z(\rho_l, \varphi_m, t_n) + E_z(\rho_{l-1}, \varphi_m, t_n)}{(\Delta \rho)^2}, \tag{4}$$

$$\frac{\partial^2 E_z}{\partial \varphi^2} \approx \frac{E_z(\rho_l, \varphi_{m+1}, t_n) - 2E_z(\rho_l, \varphi_m, t_n) + E_z(\rho_l, \varphi_{m-1}, t_n)}{(\Delta \varphi)^2},$$

where l, m, and n are integers.

Because calculations were performed for a certain finite region, the wave function at its boundaries was set equal to zero, while a signal at the input of waveguide (*8*) was written in the form

$$E_z(x_0 = 0, y, t) = E_0 \exp\left[-\frac{(y - y_0)^2}{a^2}\right] \sin(2\pi f t). \tag{5}$$

The distribution of the electromagnetic field component E_z in the interaction region of input waveguide (*8*) and closed waveguide (*9*) was calculated by the expression

$$E_z(\rho, \varphi, t) = E_1 \exp\left\{-\frac{[(\rho - \rho_0)\cos\varphi]^2}{a^2}\right\} \sin(2\pi f t), \tag{6}$$

where E_0 is the signal amplitude at the input of waveguide (*8*); E_1 is the amplitude of the signal arrived at closed waveguide (*9*); f is the carrier frequency; and the values x_0, y_0, ρ_0, $\varphi_0 = 0$, and constant a specify the shape and spatial distribution of the input signal.

Wave equation (1) was solved by specifying intervals Δx and Δy smaller than the input radiation wavelength, and the time sampling step was chosen taking into account the Courant stability condition [6]

$$\Delta t \leqslant \frac{1}{c[(1/\Delta x)^2 + (1/\Delta y)^2]^{1/2}}. \tag{7}$$

The relation between variables during the solution of wave equation (2) in cylindrical coordinates was specified similarly. The calculated resonance parameters were compared with experimental data for a ring silicon microcavity of radius 5 μm [7]. The calculated FWHM of the absorption band of the photosensitive element coincided with the experimental width within 2 %.

The composite microcavity (Fig. 1) was simulated by assuming that coefficients k_1 and k_3 of optical coupling of

input (*8*) and output (*12*) waveguides with corresponding closed waveguides (*9*) and (*10*) are equal to 0.224, while the coefficient k_2 of optical coupling between closed waveguides was chosen in the interval from 0.002 to 0.02.

The numerical simulation was performed for waveguides made of silicon with the thermal expansion coefficient of 2.5×10^{-6} K^{-1} [8] and having thickness and width 0.5 μm. The length of straight waveguides (*8*) and (*12*) was set equal to 11 μm, while the radius of closed waveguides (*9*) and (*10*) was 10 μm. The output power of laser (*7*) at input waveguide (*8*) used in all calculations was 1 mW. The parameters of the pixel were estimated by calculating its resonance transmission bands [dependences of signals E^2_{out} at the output of waveguide (*12*) on the wavelength] (Fig. 2) and dependences of the maximum values of the output optical signal and the FWHM of the resonance transmission band on the coupling coefficient k_2 between closed waveguides (*9*) and (*10*) (Fig. 3). The curves presented in Fig. 3 demonstrate a strong dependence of the output signal amplitude on the coupling coefficient k_2, which can be used to provide the equality of the output optical power for all photosensitive elements located along input waveguide (*8*). To accomplish this, the coupling coefficients k_2 should linearly change, for example, from 0.002 to 0.02. One can see from Fig. 2 that the resonance transmission band is shifted from its initial position when temperature is changed by 0.5 K. For $k_2 = 0.02$ and the output power of the waveguide laser equal to 1 mW, the linear region of the resonance transient characteristic corresponds to the change of the optical signal power by 0.28 mW. To provide the signal-to-noise ratio of no more than 16 at the output of photodetectors used in practice, the incident radiation power should be $\sim 1.85 \times 10^{-4}$ mW [4, 9]. This means that the minimal temperature change that can be detected is 3.3×10^{-4} K, which is 1.8 times greater than the limiting sensitivity of thermal imaging detectors [10]. The reading time of information from a photosensitive element is determined by the establishment time of the optical signal amplitude in output waveguide (*12*), which is 27 ps for the composite microcavity of size under study [11], and by the response time of the photodetector.

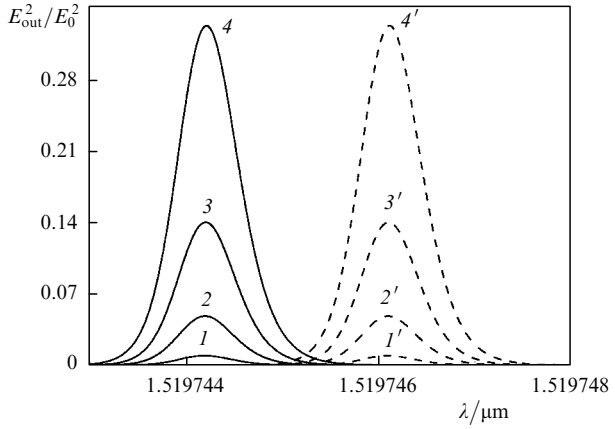

Figure 2. Resonance transmission bands of the sensitive element of the silicon IR photodetector for coupling coefficients $k_2 = 0.002$ (*1, 1′*), 0.005 (*2, 2′*), 0.01 (*3, 3′*), and 0.02 (*4, 4′*). The solid curves are transmission bands at the initial temperature of closed waveguides (*9*) and (*10*), the dashed curves are transmission bands at temperature changed by 0.5 K.

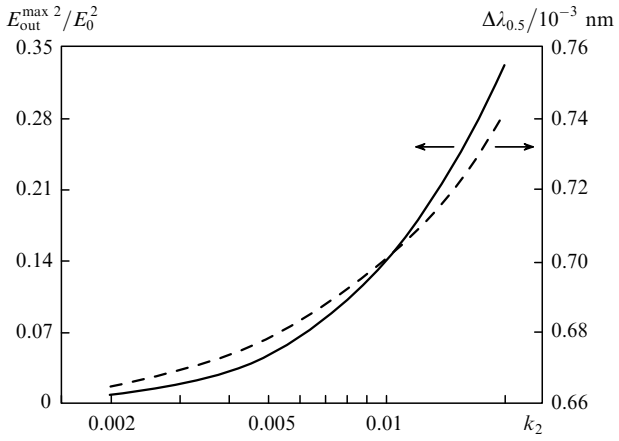

Figure 3. Dependences of the maximum values of the output signal and the FWHM of the transmission band of the photosensitive element of the IR photodetector on the coupling coefficient k_2 between closed waveguides.

To estimate the response time of a pixel to an IR signal and its threshold parameters, we analysed the transfer of thermal energy for absorbing element (*11*) to closed waveguides (*9*) and (*10*) by numerical simulations based on the one-dimensional heat conduction equation [12]

$$\rho_i c_i \frac{\partial T}{\partial t} = \frac{\partial}{\partial x}\left(k_i \frac{\partial T}{\partial x}\right) + Q(x,t), \quad i = 1, 2, \ldots, N \tag{8}$$

under boundary and initial conditions

$$\left.\frac{\partial T}{\partial x}\right|_{x=0} = 0, \quad T(x = d, t) = T_0, \quad T(x, t = 0) = T_0, \tag{9}$$

where i is the number of a layer of the photosensitive element; ρ_i, c_i and k_i are its density, heat capacity, and heat conduction, respectively; T is temperature; $Q(x,t)$ is a function of a thermal source; d is the thickness of the sensitive element; and T_0 is the initial temperature.

The temperature field in the sensitive element of the IR photodetector satisfies the conditions of joining of its elements made of different materials at interfaces $x = \xi$:

$$T_j = T_{j+1} \text{ for } x = \xi, \quad j = 1, \ldots, 4, \tag{10}$$

$$k_j \left.\frac{\partial T_j}{\partial x}\right|_{x=\xi} - k_{j+1} \left.\frac{\partial T_{j+1}}{\partial x}\right|_{x=\xi} = 0, \tag{11}$$

where the subscript $j = 1$ corresponds to absorbing element (*11*) made of niello on gold [13]; $j = 2$ and 4 corresponds to the upper and lower SiO_2 buffer layers; $j = 3$ – to closed optical silicon waveguides (*9*) and (*10*); $j + 1 = 5$ corresponds to silicon substrate (*1*); T_j and T_{j+1} are temperatures of contacting surfaces of the jth and $j + 1$th elements made of different materials; k_j and k_{j+1} are the heat conductivities of corresponding elements.

The thermal source function $Q(x,t)$ in heat conduction equation (8) describes heat release in the ith layer of the jth element during heat transfer:

$$Q(x,t) = \left\{ (1-R)\frac{P}{S_i}\alpha_i(x)\exp\left[-\int_0^x \alpha_i(x')\mathrm{d}x'\right]\right\}_j, \quad (12)$$

where R is the reflectance of absorbing element (*11*); $\alpha_i(x)$ is the absorption coefficient of the ith layer of the jth element; P is the incident IR radiation power; S_i is the area of the ith layer of the sensitive element under study.

Numerical simulation was performed for the absorbing element of thickness 2.5 μm and the heat capacity of its unit area equal to 8.368×10^{-3} J cm^{-2} K^{-1} [13]. The sizes of upper and lower buffer layers (*16*) and closed optical waveguides (*9*) and (*10*) are the same and presented above.

The dependences of the maximum temperature variations of composite microcavity (*14*) and their establishment time on the input power density $P_{\mathrm{in}}^{\mathrm{IR}}$ for different IR radiation exposure times are presented in Fig. 4. Figure 5 shows the time dependences of the temperature variation of the sensitive element for the minimal IR radiation exposure time of 1 ms and radiation power densities of $\sim 1.4\times10^{-2}$ and $\sim 2.8 \times 10^{-2}$ W cm^{-2}. In this case, the radiation power incident of each photosensitive element was 10^{-7} and 2×10^{-7} W, respectively. One can see from these dependences that the response time of the photosensitive element exposed to IR radiation and the relaxation time of this element after the termination of irradiation are 3 and 26.3 ms for power densities indicated above.

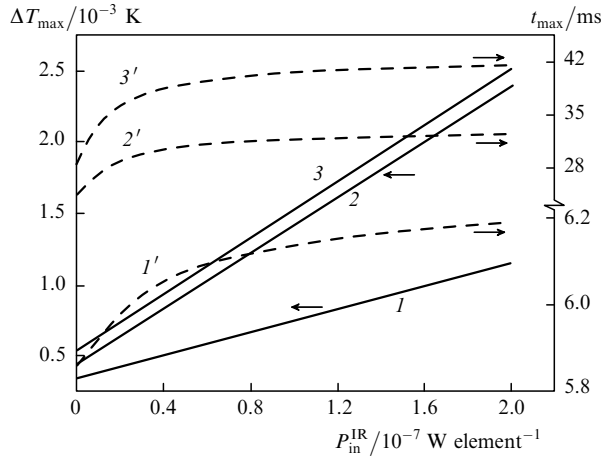

Figure 4. Dependences of the maximum temperature variations of closed waveguides (*9, 10*) and the response time on the IR radiation power $P_{\mathrm{in}}^{\mathrm{IR}}$ for radiation exposure times 1 (*1, 1′*), 20 (*2, 2′*), and 30 ms (*3, 3′*).

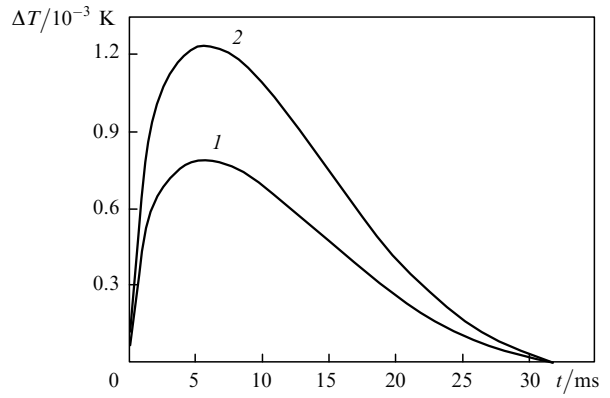

Figure 5. Time dependences of the temperature variation ΔT of closed waveguides (*9*) and (*10*) for the exposure time 1 ms and the incident IR radiation power density $P_{\mathrm{in}}^{\mathrm{IR}} = 1 \times 10^{-7}$ (*1*) and 2×10^{-7} W element^{-1} (*2*).

4. Conclusions

The expected time constant determining the response time of one photosensitive element to the IR signal variation, taking into account the response time of the photodetector, is 30 ms. Therefore, it is possible to built a microcavity array IR photodetector with the full-frame scanning rate above 30 Hz.

To achieve the temperature contrast $\sim 10^{-3}$ K, the IR radiation power density incident on the photosensitive element under study should be $\sim 16.2 \times 10^{-8}$, $\sim 5.8\times 10^{-8}$ and $\sim 4.7 \times 10^{-8}$ W for exposure times 1, 20, and 30 ms, respectively.

References

1. Tarasov V.V, Yakushenkov Yu.G. (Eds) *Optiko-elektronnye sistemy vizualizatsii i obrabotki opticheskikh izobrazhenii (sbornik statei)* (Optoelectronic Systems for Visualisation and Processing of Optical Images) (Collection of Papers) (Moscow: Izd. Altei, 2007) No. 2.
2. Lipatov N.I., Biryukov A.S. *Kvantovaya Elektron.*, **36**, 389 (2006) [*Quantum Electron.*, **36**, 389 (2006)].
3. Esman A.K., Kuleshov V.K., Zykov G.L. Patent of Belarus, No. 12232.
4. Schreiner R., Nagele P., Korbl M., et al. *IEEE Photon. Techol. Lett.*, **13**, 1277 (2001).
5. Logginov A.S., Maiorov A.Sh. Kryazhimskii S.A. *Radiotekhnika*, **1**, 24 (2005).
6. Kalitkin N.N. *Chislennye metody* (Numerical Methods) (Moscow: Nauka, 1978).
7. Xu Q., Lipson M. *Opt. Express*, **15**, 924 (2007).
8. Okada Y., Tokumaru Y. *J. Appl. Phys.*, **56**, 314 (1984).
9. Filachev A.M. Ponomarenko V.P., Taubkin I.I., et al. *Prikl. Fiz.*, **6**, 52 (2002).
10. Taubkin I.I., Trishenkov M.A. *Prikl. Fiz.*, **6**, 48 (2001).
11. Pilipovich V.A., Esman A.K., Goncharenko I.A., et al. *Dokl. Nats. Akad. Nauk Belarus.*, **52**, 48 (2008).
12. Mel'nikov A.A. *Nano- Mikrosist. Tekh.*, **2**, 21 (2000).
13. Sintsov V.N. *Zh. Prikl. Spektr.*, **4**, 503 (1966).